SAND80-1847
Unlimited Release
UC-32

Numerical Evaluation of the Transfer Impedance of Two Parallel Loop Antennas

Donald E. Amos

Prepared by Sandia National Laboratories, Albuquerque, New Mexico 87185
and Livermore, California 94550 for the United States Department
of Energy under Contract DE-AC04-76DP00789

Printed September 1980

Sandia National Laboratories

SF 2900-Q(3-80)

DISCLAIMER

Issued by Sandia Laboratories, operated for the United States Department of Energy by Sandia Corporation.

Printed in the United States of America

Available from
National Technical Information Service
5285 Port Royal Road
Springfield, Virginia 22161
Price: Printed Copy $4.00; Microfiche $3.00

SAND80-1847
Unlimited Release
Printed September 1980

UC-32

Numerical Evaluation of the Transfer Impedance of Two Parallel Loop Antennas

D. E. Amos
Numerical Mathematics Div. 5642
Sandia National Laboratories
Albuquerque, NM 87185

Abstract

A Fourier integral representation of the complex transfer impedance of two parallel loop antennas of radius a, separated on a common axis by a distance d, is converted into an integral I_1 whose integrand decays exponentially. This integral is further manipulated to produce a series representation which can be used numerically when $d \geq 3a$. A second integral I_2, whose integrand also decays exponentially, is derived and, like I_1, converges for $d > 0$. While a quadrature on I_1 can be performed when $d < 3a$, the quadrature requires evaluations of the J_1 Bessel function of a complex argument. However, the integrand of I_2 requires only elementary functions of complex arguments and the J_1 Bessel function of real arguments. Consequently, a quadrature on I_2 for $d < 3a$ is recommended to complement the series evaluation for $d \geq 3a$.

Introduction

The formula

$$I(d) = \int_0^\infty J_1(w)H_1^{(2)}(w) \cos \zeta d \, d\zeta , \qquad w = a\sqrt{k^2-\zeta^2} \tag{1}$$

$$k = k_1 - ik_2, \; k_1 > 0, \; k_2 > 0, \; a > 0, \; d > 0$$

where J_1 and $H_1^{(2)}$ are Bessel functions is developed in [3] to express the complex transfer impedance of two parallel loop antennas of radius a separated by a distance d on a common axis. The transfer impedance relates the open circuit voltage V induced in the receiving loop to the current I_t in the transmitting loop by $I(d) = V/I_t$. The object of this manuscript is to derive two representations which can be used to evaluate I numerically for the calculations in [5]. The necessity for alternate representations comes about because the convergence rate in (1) is too slow to obtain accurate answers by numerical integration. The integral (1) is only conditionally convergent with an integrand which decreases slowly like $O(|\zeta|^{-1})$. This means that a quadrature must extend over several orders of magnitude to reduce the truncation error to acceptable levels, and this means unacceptable computer costs.

The key to this development is to note that (1) can be written as a two sided Fourier transform

$$I = \frac{1}{2}\int_{-\infty}^{+\infty} J_1(w) \, H_1^{(2)}(w) \, e^{-id\zeta} \, d\zeta \tag{2}$$

and this can be converted into a Laplace transform with an exponentially decaying integrand. This is done by applying Cauchy's theorem to the integral in the complex ζ plane

$$\int_C J_1(w)\, H_1^{(2)}(w)\, e^{-i\zeta d}\, d\zeta\,, \qquad w = a\sqrt{k^2-\zeta^2} \qquad (3)$$

along the paths of Figures 1 and 2 with $R \to \infty$. The path in Figure 1 leads to an integral I_1, valid for $d > 0$, in terms of J_1 of a complex argument. I_1 can be further manipulated to produce a series representation which, though convergent for $d > 2a$, is suitable for numerical evaluation for d much larger than 2a, say $d \geq 3a$. The path in Figure 2 leads to an integral solution I_2 which, like I_1, converges for $d > 0$ but expresses the solution in terms of elementary complex functions and real J_1 Bessel functions. Consequently a quadrature on I_2 is recommended for computation when $d < 3a$.

Solution I_1

The plan is to apply Cauchy's theorem to (3) along the contour of Figure 1. For the reduction, we show that the integrals along C_1 through C_4 vanish as $R \to \infty$. Then, $2I_1$, the integral from X_1 to X_2 along the axis, must be equal to the integral around C_5 as $R \to \infty$.

Before we start the estimation of integrals, we need a careful analysis of the phases associated with the branch

$$\sqrt{k^2-\zeta^2} = \sqrt{k+\zeta}\,\sqrt{k-\zeta} = \sqrt{R_1R_2}\, e^{i(\varphi_1+\varphi_2)/2}$$

$$k - \zeta = R_1 e^{i\varphi_1}\,, \quad k+\zeta = R_2 e^{i\varphi_2}$$

where k is a fourth quadrant complex number. The geometric relationships are shown in Figure 3. Note that the magnitude of the argument of the factor $k-\zeta$ has a jump of 2π in traversing from a point on one side of a cut to the corresponding point on the other side. This means that $\arg(\sqrt{k^2-\zeta^2}) = (\varphi_1+\varphi_2)/2$ has a jump of magnitude π in moving (continuously) from one side to the other.

We also note, for future reference, the behavior of $J_1(z)$ and $H_1^{(2)}(z)$ in the complex z plane for small and large $|z|$ [1, p. 360, 364],

$$J_1(z) = \frac{z}{2} + O\left(\frac{|z|^2}{2}\right) \qquad H_1^{(2)}(z) = \frac{1}{\pi}\cdot\frac{2}{z} + O\left(\frac{|z|}{2}\ln\frac{|z|}{2}\right)$$

$$|z| \to 0, \quad |\arg z| < \pi \qquad (4)$$

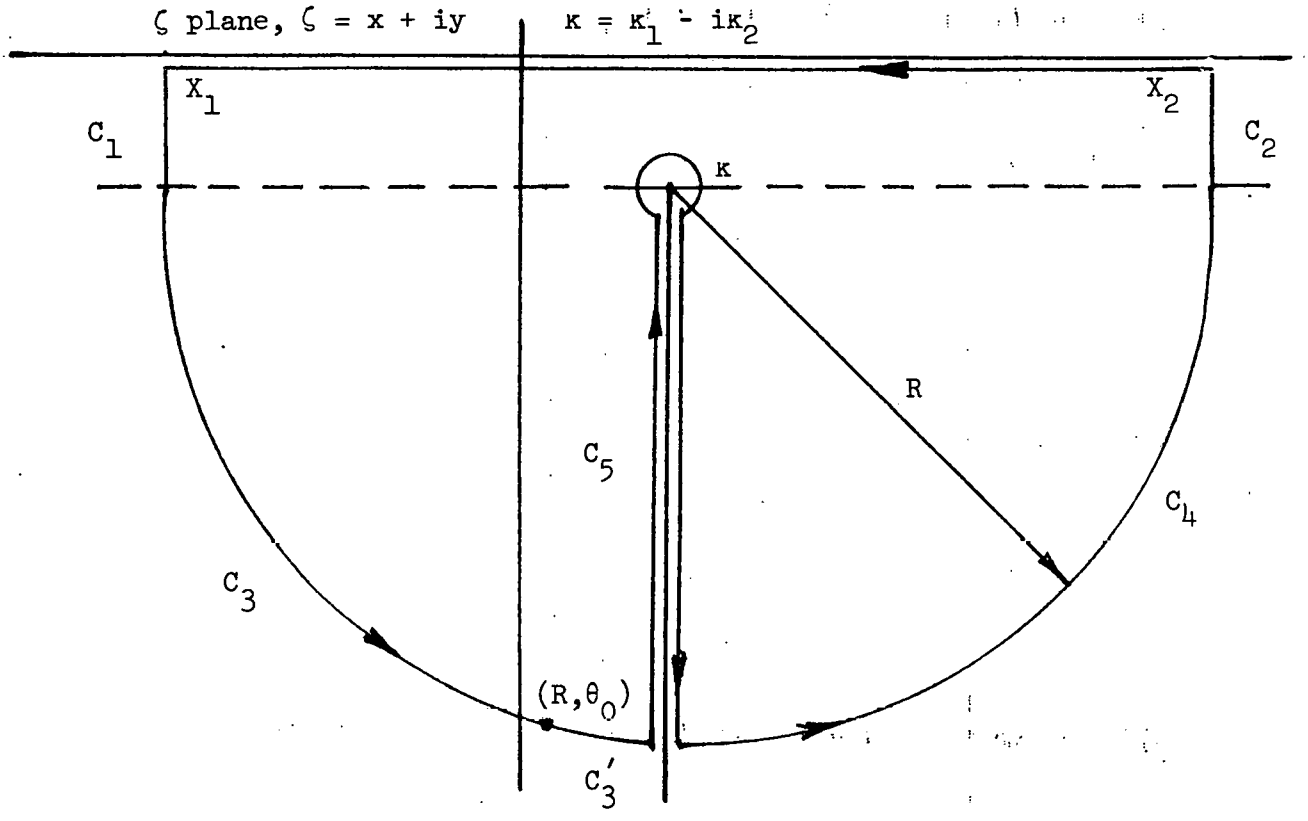

Figure 1.

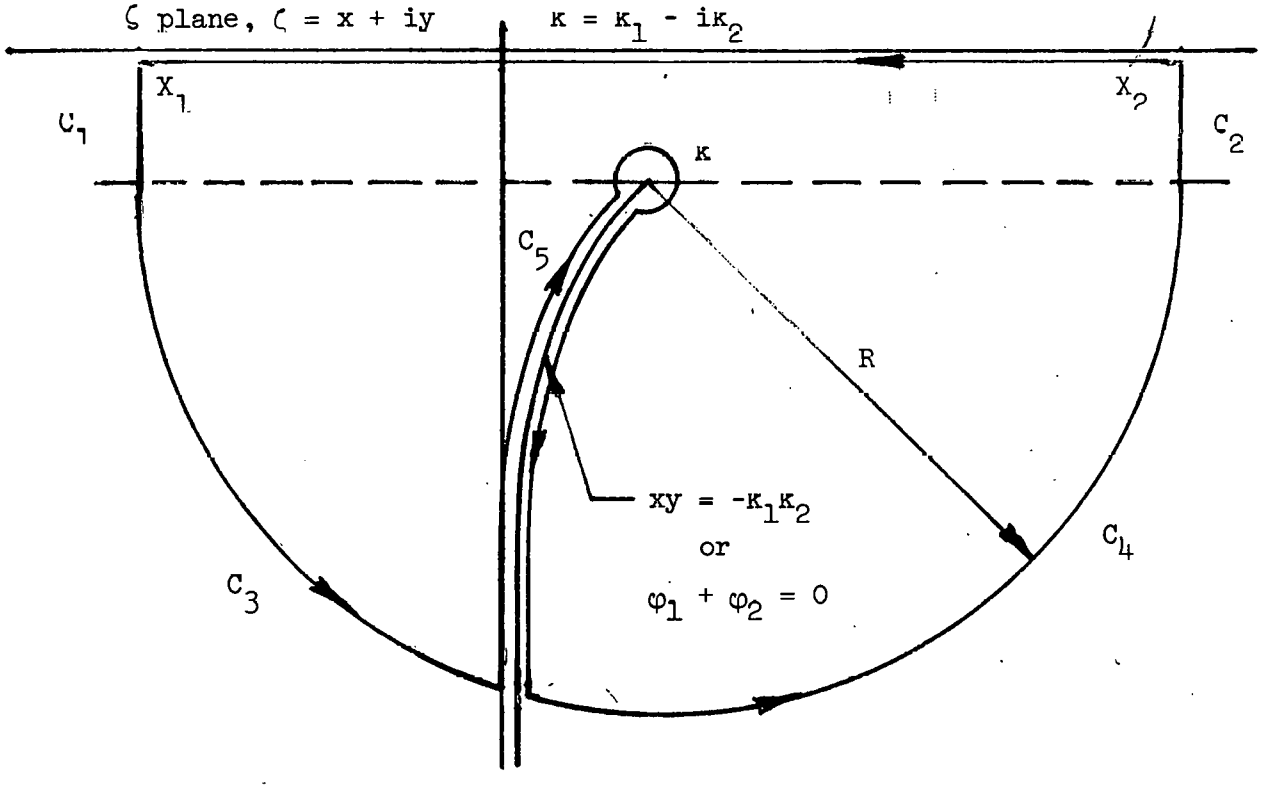

Figure 2.

Arguments of $\kappa + \zeta$ and $\kappa - \zeta$

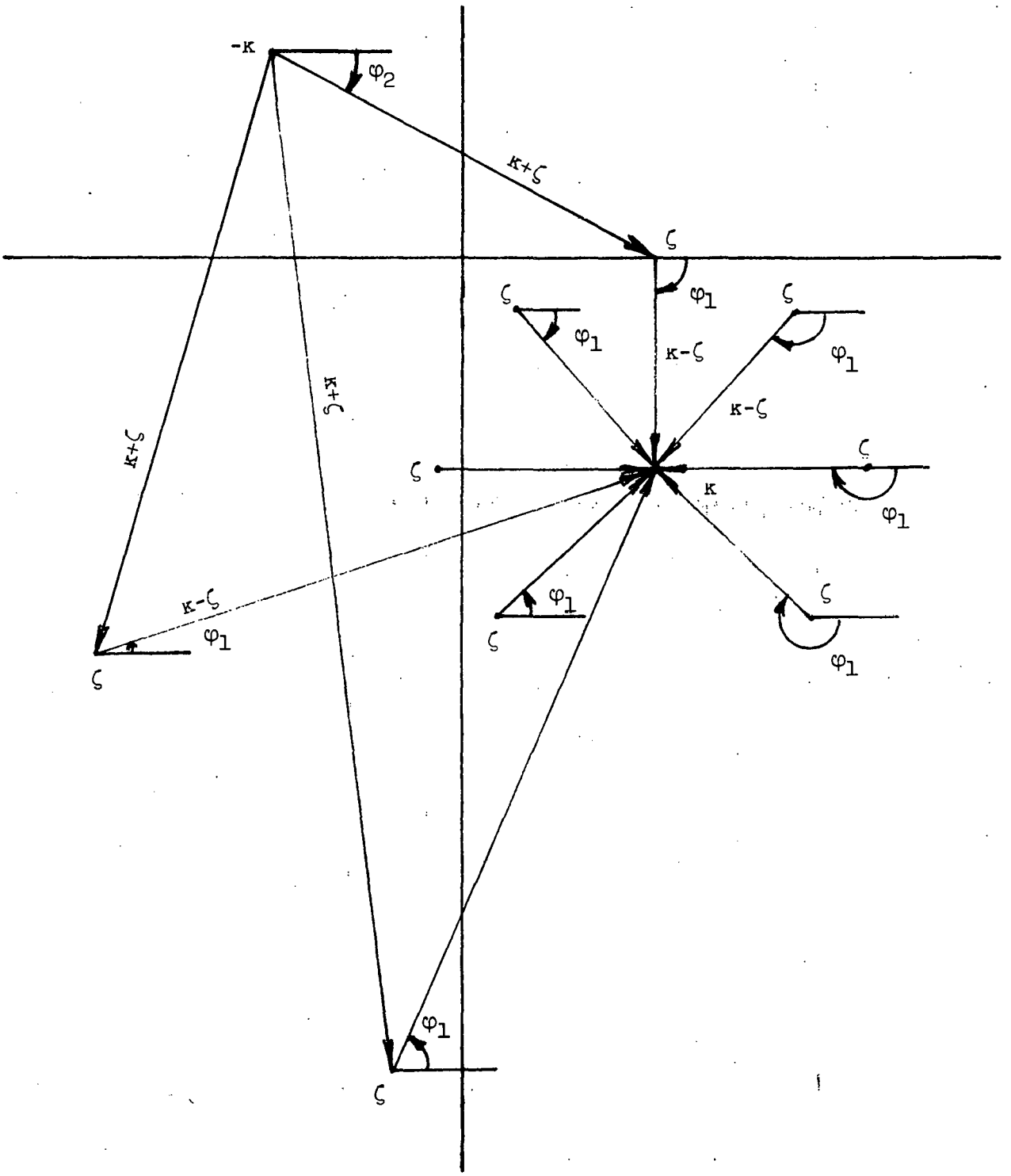

$$\kappa + \zeta = R_2 e^{i\varphi_2}, \quad \kappa - \zeta = R_1 e^{i\varphi_1}$$

Figure 3.

$$J_1(z) = \sqrt{\frac{2}{\pi z}} \left\{ \cos\,(z - 3\pi/4) + e^{|\mathrm{Im}(z)|} O(|z|^{-1}) \right\}$$

$$H_1^{(2)}(z) = \sqrt{\frac{2}{\pi z}}\ e^{-i(z-3\pi/4)} \left\{ 1 + O(|z|^{-1}) \right\}$$

$$|z| \to \infty\ ,\ |\arg z| < \pi\ .$$

Case I, Contours C_1 and C_2 of Figure 1

We bound the integrals on C_1 and C_2 by the triangle inequality, using $\zeta = X_1 + iy$ and $\zeta = X_2 + iy$. Then,

$$\left| \int_{C_j} \right| \leq \int_0^{k_2} |J_1|\ |H_1^{(2)}|\ e^{yd}\, dy\ , \qquad j = 1,2$$

where $|J_1(w)|\ |H_1^{(2)}(w)|$ is evaluated on C_j for large X_j. The asymptotic estimates (4) along with

$$|\cos\,(z-3\pi/4)|^2 = \cos^2\,(x-3\pi/4) + \sinh^2 y \sim \frac{e^{2|y|}}{4}$$

show that $|J_1|$ and $|H_1^{(2)}|$ are bounded by

$$\sqrt{\frac{2}{\pi}}\ \frac{K_1\ \exp[a\sqrt{R_1R_2}\,|\sin\frac{\varphi_1+\varphi_2}{2}|]}{\sqrt{a\sqrt{R_1R_2}}} \quad \text{and} \quad \sqrt{\frac{2}{\pi}}\ \frac{K_2\ \exp[a\sqrt{R_1R_2}\,\sin\ \frac{(\varphi_1+\varphi_2)}{2}]}{\sqrt{a\sqrt{R_1R_2}}}$$

respectively for large R where $R_1 = O(|X_j|)$, $R_2 = O(|X_j|)$. Here K_1 and K_2 were inserted to convert asymptotic estimates into rigorous inequality. Then,

$$|J_1|\ |H_1^{(2)}| \leq \frac{2}{\pi}\ \frac{K_1K_2\ \exp\left\{a\sqrt{R_1R_2}\left[|\sin\ \frac{(\varphi_1+\varphi_2)}{2}| + \sin\ \frac{(\varphi_1+\varphi_2)}{2}\right]\right\}}{a\sqrt{R_1R_2}} \qquad (5)$$

From Figure 3 we see that $-\pi - \epsilon < \varphi_1 + \varphi_2 < 0$ where ϵ is small and positive when R, and consequently R_1, R_2, X_1 and Y_2, is large. Then,

$$\frac{-\pi}{2} - \frac{\epsilon}{2} < \frac{\varphi_1+\varphi_2}{2} < 0$$

and the exponential in (5) becomes 1. Therefore, $|J_1|\ |H_1^{(2)}|$ is bounded by quantities which decrease like $O(|X_j|^{-1})$ for $X_1 \to -\infty$ and $X_2 \to \infty$. Since exp (yd) is bounded on $0 \le y \le k_2$, the integrals along C_1 and C_2 vanish as $|X_1| \to \infty$ or $|X_2| \to \infty$.

Case II, Contours C_3 and C_4 of Figure 1

We first treat the case for C_4 in Figure 1 with ζ on the semi-circular contour

$$\zeta = k + R\, e^{i\theta} = k + R\,(\cos\theta + i \sin\theta).$$

The triangle inequality produces

$$\left|\int_{C_4}\right| \le |e^{-ikd}| \int_{-\pi/2}^{0} R\ |J_1|\ |H_1^{(2)}|\ e^{Rd\sin\theta} d\theta.$$

The estimate in (5) still applies for $|J_1(w)|\ |H_1^{(2)}(w)|$ on C_4 since the arguments w of the Bessel functions have a phase $(\varphi_1+\varphi_2)/2$ satisfying

$$-\pi < \frac{\varphi_1+\varphi_2}{2} < \frac{-\pi}{2}$$

within the permissible range $|\arg w| < \pi$. This can be seen from Figure 3 by noting the relations $-\pi/2 < \varphi_2 < 0$ and $-3\pi/2 < \varphi_1 < -\pi$. Thus, the argument of the exponential function in (5) is zero and

$$|J_1|\ |H_1^{(2)}| \le \frac{2K_1K_2}{\pi a\sqrt{R_1R_2}}$$

on C_4. Then, with $\zeta = k + R\, e^{i\theta}$ and $R_1 = R$, we have

$$\left|\int_{C_4}\right| \le \frac{2K_1K_2|e^{-ikd}|}{\pi a} \int_{-\frac{\pi}{2}}^{0} \frac{R}{\sqrt{R_1R_2}}\ e^{Rd\sin\theta} d\theta$$

where $R/\sqrt{R_1R_2} = \sqrt{R/R_2}$ is bounded by 1. Therefore it remains to verify that

$$\lim_{R\to\infty} \int_{-\frac{\pi}{2}}^{0} e^{Rd\sin\theta} d\theta = 0.$$

A change of variables $\sin\theta = -x$ gives

$$f(R) = \int_{-\frac{\pi}{2}}^{0} e^{Rd\sin\theta} d\theta = \int_{0}^{1} \frac{e^{-Rdx}\, dx}{\sqrt{1-x^2}}$$

and Watson's lemma shows that $f(R)$ decreases like $O(|Rd|^{-1})$ for $R \to \infty$.

The contour C_3 to the left of the imaginary axis is much like that for C_4 in the portion where $-\pi/2 < (\varphi_1+\varphi_2)/2 \leq 0$. The point (R,θ_0) at which $(\varphi_1+\varphi_2)/2 = 0$ occurs to the right of the imaginary axis since, on the axis, we have (see Figure 4)

$$\cos|\varphi_2| = \frac{h_2}{2R_2} < \frac{h_2}{2R} = \cos\varphi_1$$

which implies $|\varphi_2| > \varphi_1$ and $\sin\dfrac{(\varphi_1+\varphi_2)}{2} = \sin\dfrac{(\varphi_1-|\varphi_2|)}{2} < 0$. But, on the left side of the cut, $\varphi_1 = \pi/2$ and $|\varphi_2| < \pi/2$. Thus, $(\varphi_1 - |\varphi_2|)/2 = (\varphi_1+\varphi_2)/2$ can be positive which, according to (5), leads to an exponentially increasing estimate

$$|J_1|\,|H_1^{(2)}| \leq \frac{2K_1K_2}{\pi a\sqrt{R_1R_2}} \exp\left\{2a\sqrt{R_1R_2}\sin\frac{(\varphi_1+\varphi_2)}{2}\right\}.$$

However, this is mitigated by the fact that the exponential

$$|e^{-id\zeta}| = |e^{-ikd}|e^{Rd\sin\theta} \qquad \pi \leq \theta \leq \frac{3\pi}{2}$$

is decreasing. Since $\varphi_1 \to \pi/2$ and $\varphi_2 \to -\pi/2$ for $R \to \infty$ with ζ on the left side of the cut, $\sin(\varphi_1+\varphi_2)/2 \to 0$ and $\sqrt{R_1R_2}\sin(\varphi_1+\varphi_2)/2$ is indeterminant as $R \to \infty$. To resolve this indeterminacy we use the geometry of Figure 4. We have

$$\sin |\varphi_2| = \frac{h_1 + R \sin \varphi_1}{R_2}, \quad \cos |\varphi_2| = \frac{h_2 - R \cos \varphi_1}{R_2}, \quad R = R_1$$

$$\sin \frac{\varphi_1+\varphi_2}{2} = \sin \frac{(\varphi_1 - |\varphi_2|)}{2} = \sqrt{\frac{1 - \cos (\varphi_1 - |\varphi_2|)}{2}}$$

$$= \sqrt{\frac{R_2 - R \cos 2\varphi_1 - (h_2 \cos \varphi_1 + h_1 \sin \varphi_1)}{2R_2}}$$

$$\varphi_1 = \theta - \pi$$

$$\sin \frac{(\varphi_1+\varphi_2)}{2} = \sqrt{\frac{1 - \cos 2\theta}{2} - \frac{h_2 \cos \varphi_1 + h_1 \sin \varphi_1}{R_2} + \left(1 - \frac{R}{R_2}\right) \cos 2\theta}$$

$$\sim \sqrt{\frac{1-\cos 2\theta}{2}} = - \sin \theta \qquad \text{for } R \to \infty$$

Now, $R_1 = R$ and $R_2 \to R$ as $R \to \infty$ and

$$|J_1| \; |H_1^{(2)}| \; e^{Rd\sin\theta} \leq \frac{2K_1K_2}{\pi a R} \exp \{R(d-2a)\sin \theta\}$$

on C_3'. Then,

$$\left| \int_{C_3'} \right| \leq \frac{2K_1K_2 |e^{-ikd}|}{\pi a} \int_{\theta_0}^{3\pi/2} \frac{e^{(d-2a)R\sin\theta}}{R} Rd\theta.$$

Since $\sin \theta < 0$ on $\theta_0 \leq \theta \leq 3\pi/2$, we can make the bound vanish if $d > 2a$ and $R \to \infty$.

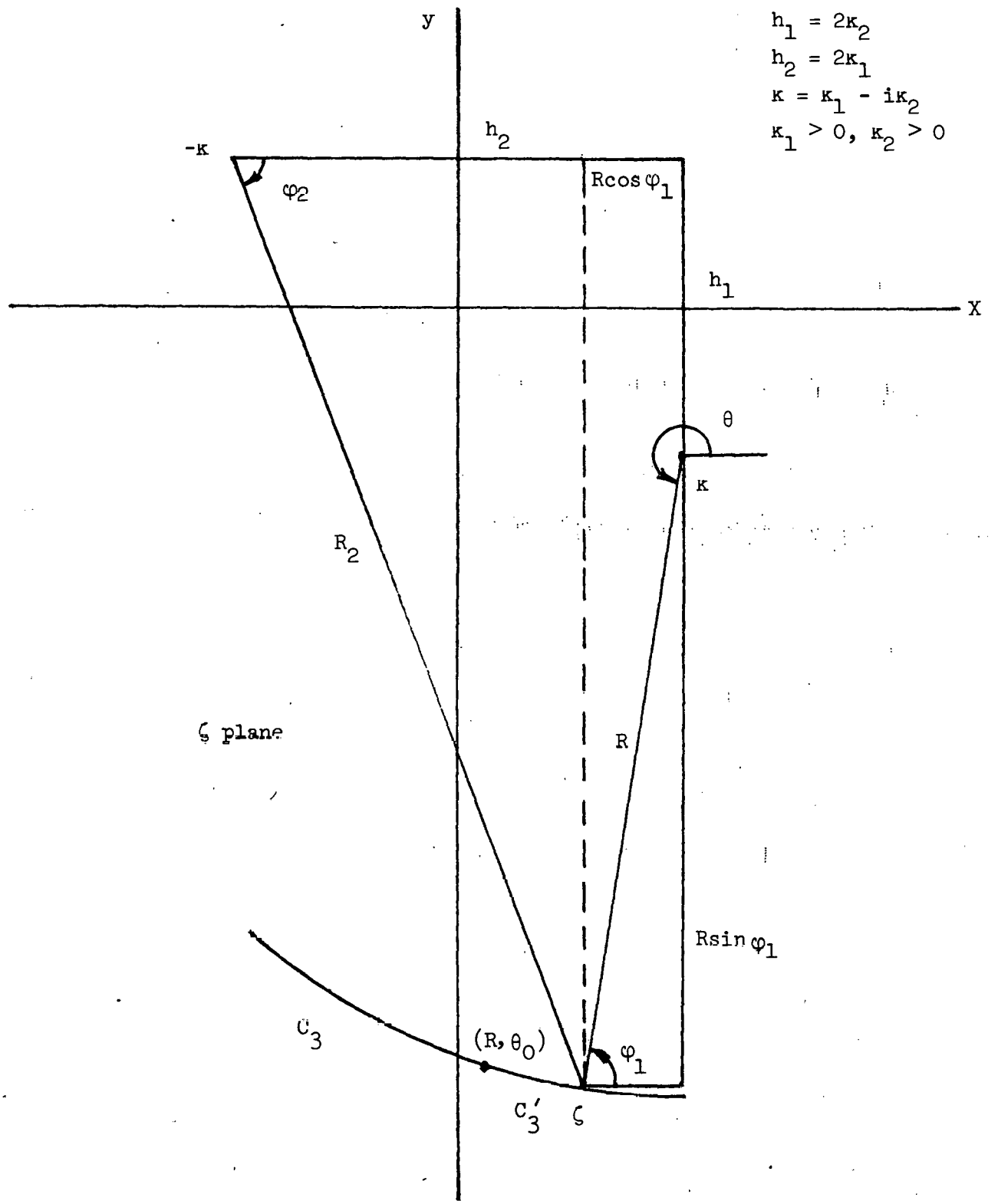
y
$h_1 = 2\kappa_2$
$h_2 = 2\kappa_1$
$\kappa = \kappa_1 - i\kappa_2$
$\kappa_1 > 0,\ \kappa_2 > 0$
h_2
$-\kappa$
φ_2
$R\cos\varphi_1$
h_1
X
θ
κ
R_2
ζ plane
R
$R\sin\varphi_1$
C_3
(R, θ_0)
φ_1
C_3'
ζ

Figure 4.

Case III, Contour C_5 of Figure 1

We first show that the integral about the circle

$$|k-\zeta| = r$$

at the top of the keyhole in Figure 1 vanishes as $r \to 0$. With $\zeta = k + re^{i\theta}$, $-\pi/2 < \theta < 3\pi/2$, we get

$$J_1(a\sqrt{k^2-\zeta^2}) = J_1(a\, e^{i\theta/2}\, \sqrt{r}\, \sqrt{2k+re^{i\theta}})$$

$$H_1^{(2)}(a\sqrt{k^2-\zeta^2}) = H_1^{(2)}(ae^{i\theta/2}\, \sqrt{r}\sqrt{2k+re^{i\theta}})$$

where the arguments are small for small r. We therefore need the behavior of $J_1(z)$ and $H_1^{(2)}(z)$ for small $|z|$ from (4),

$$J_1(z) \sim \frac{z}{2}\ , \qquad H_1^{(2)}(z) \sim \frac{1}{\pi} \cdot \frac{2}{z}\ .$$

Thus, $|J_1|\ |H_1^{(2)}| \sim 1/\pi$ remains bounded and

$$\left|\int_{\odot}\right| \le \frac{K}{\pi} \int_{3\pi/2}^{-\pi/2} |e^{-ikd}|\ e^{rd\sin\theta}\ |rie^{i\theta}|d\theta$$

$$\le \frac{K}{\pi}\ \ r\ |e^{-ikd}| \int_{3\pi/2}^{-\pi/2} e^{rd\sin\theta}\ d\theta.$$

This estimate shows that the integral around the circle vanishes as $r \to 0$.

The integrals along each side of the branch cut are not the same because the argument w of $J_1(w)\ H_1^{(2)}(w)$ is discontinuous. We consult Figure 3 to get the correct phase of

$$w = a\sqrt{k^2-\zeta^2} = a\sqrt{R_1R_2}\ e^{i(\varphi_1+\varphi_2)/2}.$$

Thus, the contour about C_5 reduces to

$$2I_2 = e^{-ikd}\left\{\int_{\infty}^{0} J_1(\beta)H_1^{(2)}(\beta)e^{-rd}(-i)dr + \int_{0}^{\infty} J_1(\alpha)H_1^{(2)}(\alpha)\ e^{-rd}\ (-i)\ dr\right\}$$

where

$$\alpha = a \exp(-3\pi i/4) \sqrt{r}\sqrt{2k-ir}$$

$$\beta = a \exp(\pi i/4) \sqrt{r}\sqrt{2k-ir}.$$

Notice that $\alpha = \beta\, e^{-i\pi}$ (a jump in $(\varphi_1+\varphi_2)/2$ of $-\pi$) and the analytic continuation formulae

$$J_1(z\, e^{-i\pi}) = -J_1(z)$$
$$Y_1(z\, e^{-i\pi}) = -Y_1(z) + 2iJ_1(z)$$

together with the definition of $H_1^{(2)}(z)$

$$H_1^{(2)}(z) = J_1(z) - i\, Y_1(z)$$

give

$$J_1(z\, e^{-i\pi}) = -J_1(z)$$
$$H_1^{(2)}(z\, e^{-i\pi}) = J_1(z) + i\, Y_1(z)\,. \tag{6}$$

Then, $2I$ reduces to

$$2I_1 - 2i\, e^{-ikd} \int_0^\infty e^{-rd}\, J_1^2(\beta)\, dr$$

and

$$I_1(d) = i\, e^{-ikd} \int_0^\infty e^{-rd}\, J_1^2\left(a\sqrt{r^2+2kir}\right) dr.$$

Under a change of variables, $ar = u$, we have

$$I_1 = \frac{i\, e^{-ikd}}{a} \int_0^\infty e^{-ud/a}\, J_1^2\left(\sqrt{u^2+2kaiu}\right) du. \tag{7}$$

While the derivation demanded that $d > 2a$, this integral is valid for $d > 0$ and represents the analytic continuation of the solution I_1 into the region $d \le 2a$. A numerical quadrature of (7) requires evaluation of J_1 for complex arguments which can be obtained from [2].

However, there is an additional manipulation which yields a convergent series. The series expansion for $J_1^2(z)$ is [4, p. 97].

$$J_1^2(z) = \sum_{m=0}^{\infty} a_m z^{2m+2} \quad , \quad a_m = \frac{(-1)^m (2m+2)!}{m!(m+2)![(m+1)!]^2 2^{2m+2}}$$

and

$$J_1^2 (\sqrt{u^2+2kaiu}) = \sum_{m=0}^{\infty} a_m [u^2+2kaiu]^{m+1} .$$

Then,

$$I = \frac{i\, e^{-ikd}}{a} \sum_{m=0}^{\infty} a_m \int_0^{\infty} e^{-ud/a} [u^2+2kaiu]^{m+1} du.$$

This integral is a Laplace transform of the form

$$\int_0^{\infty} e^{-pt}(t^2+2\alpha t)^{\nu-1/2} dt = \frac{\Gamma(\nu+1/2)}{\sqrt{\pi}} \left(\frac{2\alpha}{p}\right)^{\nu} e^{\alpha p} K_{\nu}(\alpha p) \qquad \begin{matrix} |\arg \alpha| < \pi \\ \text{Re } \nu > -1/2 \end{matrix}$$

where K_ν is the Modified Bessel function of the second kind. This gives

$$I = \frac{i}{a\sqrt{\pi}} \sum_{m=0}^{\infty} b_m \left(\frac{2ka^2 i}{d}\right)^{m+3/2} K_{m+3/2}(kdi)$$

where

$$b_m = a_m \Gamma(m+2) = \frac{(-1)^m (2m+2)!}{m!(m+2)!(m+1)! \cdot 2^{2m+2}}$$

$$= \frac{(-1)^m \Gamma(2m+3)}{\Gamma(m+1)\Gamma(m+2)\Gamma(m+3) \cdot 2^{2m+2}}.$$

The Legendre formula

$$\Gamma(2z) = \frac{2^{2z-1}}{\sqrt{\pi}} \Gamma(z)\, \Gamma(z+1/2)$$

reduces b_m to

$$b_m = \frac{(-1)^m\, \Gamma(m+3/2)}{\sqrt{\pi}\, \Gamma(m+1)\, \Gamma(m+3)} .$$

Notice that $K_{m+3/2}(z)$ is related to spherical Bessel functions

$$h^{(1)}_{m+1}(z) = -i\sqrt{\frac{2}{\pi z}}\; e^{-\pi i(m+3/2)/2} K_{m+3/2}(-iz)$$

$$h^{(2)}_{m+1}(z) = i\sqrt{\frac{2}{\pi z}} = e^{\pi i(m+3/2)/2}\; K_{m+3/2}(iz).$$

Numerically, the functions $K_{m+3/2}(z)$ can be generated by forward recursion on

$$K_{\nu+1}(z) = \frac{2\nu}{z}K_{\nu}(z) + K_{\nu-1}(z)$$

starting with $\nu = 1/2$ and the functions

$$K_{-1/2}(z) = K_{1/2}(z) = \sqrt{\frac{2}{\pi z}}\, e^{-z}, \qquad \mathrm{Re}\; z > 0.$$

Thus, the final form is

$$I = \frac{i}{a\sqrt{2\pi}} \left(\frac{ka^2 i}{d}\right)^{\frac{3}{2}} \sum_{m=0}^{\infty} C_m(d)\, K_{m+3/2}\,(kdi) \qquad (8)$$

where $\mathrm{Re}(kdi) > 0$ and

$$C_m(d) = \frac{(-1)^m(2m+2)!}{m!(m+1)!(m+2)!} \left(\frac{ka^2 i}{2d}\right)^m.$$

C_m can also be generated numerically by the recursion,

$$C_0 = 1$$

$$C_{m+1} = -C_m \cdot \frac{(2m+3)}{(m+1)(m+3)} \cdot \left(\frac{ka^2 i}{d}\right).$$

The rate of convergence of the series can be determined from the asymptotic expansion of $K_{m+3/2}$ for large m,

$$K_{m+3/2}(z) \sim \frac{\Gamma(m+3/2)}{2} \left(\frac{2}{z}\right)^{m+3/2}.$$

Then,

$$b_m \left(\frac{2ka^2 i}{d}\right)^{m+3/2} K_{m+3/2}(ikd) \sim \frac{(-1)^m}{2\sqrt{\pi}} \frac{\Gamma(m+3/2)}{\Gamma(m+1)} \cdot \frac{\Gamma(m+3/2)}{\Gamma(m+3)} \left(\frac{4a^2}{d^2}\right)^{m+3/2}$$

$$\sim \frac{(-1)^m}{2\sqrt{\pi}} \frac{1}{m} \left(\frac{2a}{d}\right)^{2m+3}$$

using the asymptotic form [1, p. 257]

$$\frac{\Gamma(z+a)}{\Gamma(z+b)} \sim z^{a-b} \qquad \text{for } z \to \infty.$$

This shows that the series converges provided $d > 2a$, and this form is recommended when $2a/d$ is much less than 1 where the series converges rapidly. $d \geq 3a$ or $2a/d \leq 2/3$ generally suffices for errors $O(10^{-8})$ in 20 terms.

Solution I_2

Many of the details associated with integration of (3) along contours C_1 through C_4 and the small circle around $\zeta = k$ of Figure 2 are similar to those encountered in obtaining the solution I_1. The cut $xy = -k_1 k_2$ in Figure 2 is determined so that exponential growth does not occur in the product $|J_1|\ |H_1^{(2)}|$ as it did in solution I_1 along C_3' of Figure 1. Since

$$|J_1|\ |H_1^{(2)}| \sim \frac{2}{\pi a\sqrt{R_1 R_2}} e^{a\sqrt{R_1 R_2}\left[\left|\sin\left(\frac{\varphi_1+\varphi_2}{2}\right)\right| + \sin\frac{\varphi_1+\varphi_2}{2}\right]}$$

the exponential growth is removed if

$$-\pi < \frac{\varphi_1+\varphi_2}{2} \leq 0$$

on either side of the cut. This is possible since $\varphi_1+\varphi_2$ varies on the extreme left in Figure 3 from $-\pi$ to near zero on the imaginary axis when R_1 and R_2 are large. Then, $(\varphi_1+\varphi_2)/2 = 0$ yields

$$\mathrm{Im}\left(\sqrt{(k+\zeta)(k-\zeta)}\right) = \sqrt{R_1 R_2} \sin\frac{\varphi_1+\varphi_2}{2} = 0$$

and

$$\mathrm{Im}[(k_1 - ik_2 + x + iy)(k_1 - ik_2 - x - iy)] = 0$$

produces

$$xy = -k_1 k_2.$$

Thus, $\arg(\sqrt{k^2-\zeta^2}) = (\varphi_1+\varphi_2)/2$ on the left of the hyperbola $xy = -k_1k_2$ is zero and the argument on the right is π less. The parameterization for the single valued functions on the cut is

$$\zeta = \frac{-k_1k_2}{y} + iy \ , \qquad -\infty < y < -k_2. \quad (9)$$

This construction automatically makes the exponential in the bound (5) equal to 1 and keeps the product $R|J_1|\ |H_1^{(2)}|$ bounded on C_3 and C_4. This in turn makes the integrals on C_3 and C_4 vanish as $R \to \infty$ because $|\exp(-i\zeta d)|$ decreases exponentially. Finally, $2I_2$ is the contour integral on each side of the cut,

$$2I_2 = \int_{-\infty}^{-k_2} J_1(\beta)H_1^{(2)}(\beta)\ \exp\left\{\frac{k_1k_2di}{y} + yd\right\}\zeta'(y)dy$$

$$+ \int_{-k_2}^{-\infty} J_1(\beta e^{-i\pi})H_1^{(2)}(\beta e^{-i\pi})\exp\left\{\frac{k_1k_2di}{y} + yd\right\}\zeta'(y)dy$$

and, using the jump relations (6), we get

$$I_2 = \int_{-\infty}^{-k_2} \exp\left\{\frac{k_1k_2di}{y} + yd\right\}\ J_1^2(\beta)\ \zeta'(y)\ dy$$

where

$$\zeta'(y) = \frac{k_1k_2}{y^2} + i \ , \qquad \beta = a\sqrt{R_1R_2}$$

$$R_1 = |k-\zeta| = \sqrt{k_1^2(1+k_2/y)^2 + (k_2+y)^2}$$

$$R_2 = |k+\zeta| = \sqrt{k_1^2(1-k_2/y)^2 + (k_2-y)^2}.$$

A change of variables, $y = -k_2-v$ gives

$$I_2 = e^{-k_2d}\int_0^{\infty} \exp\left[\frac{-k_1k_2\,di}{k_2+v}\right]\ e^{-vd}J_1^2(\rho)\ \left[\frac{k_1k_2}{(k_2+v)^2}+i\right]\ dv \qquad (10a)$$

$$\rho = a\sqrt{R_1R_2} = a\sqrt{|k-\zeta|\ |k+\zeta|}$$

$$\zeta = \frac{k_1k_2}{k_2+v} - i(k_2+v) \ , \qquad k = k_1-ik_2$$

and this integral converges for $d > 0$ since J_1 is real and bounded. Since the Bessel function J_1 is real, the integrand is easier to compute than that in (7), and I_2 is recommended for numerical quadrature.

For numerical purposes, we write (10a) in an alternate form

$$I_2 = e^{-kdi} \int_0^\infty \exp\left[\frac{k_1 dvi}{k_2+v}\right] e^{-vd} J_1^2(\rho) \left[\frac{k_1 k_2}{(k_2+v)^2} + i\right] dv \qquad (10b)$$

by multiplying and dividing by $\exp(k_1 di)$. In this form, we can assess not only the exponential decay, but also the local frequencies of J_1 and the trigonometric terms. Thus, we integrate on v in steps

$$\Delta v = \min\left\{\frac{3}{d}, \frac{2\pi}{A}, c\right\}, \quad c = \max\{\bar{c}, 0.1\}, \quad A = a\sqrt{2k_2+v_L}\left(\frac{k_1^2}{(k_2+v_L)^2} + 1\right)$$

$$\bar{c} = \begin{cases} \dfrac{2\pi(k_2+v_L)}{k_1 d}, & k_1 \neq 0 \\ 2\pi, & k_1 = 0 \end{cases}$$

to obtain the proper scale of integration where v_L is the lower limit of integration of each step. Notice that when $k_1 d$ is large and k_2 small, the trigonometric terms oscillate with a very high frequency near the origin $v = 0$. This means that one ought to use an adaptive quadrature routine to minimize the possibility of false results. A Gauss routine is preferable to avoid evaluation at $v = 0$ when $k_2 = 0$.

This integral was evaluated by a Gauss numerical (adaptive) quadrature routine on the real and imaginary parts of the integrand and compared with the I_1 solution. The agreement where the series converged rapidly, $d/2a > 2$, was at least as good as the tolerance used to compute I_1 and I_2. Numerical checks were also made using (7) for $d \leq 2a$ with similar agreement.

Cases for $k_1 = 0$ and $k_2 = 0$:

If $k_1 \to 0$, then the hyperbolic cut $xy = -k_1 k_2$ degenerates into a portion of the imaginary axis $\zeta = iy$, $-\infty < y \leq -k_2$, and the parameterization in (9) reflects this to give a correct evaluation in (10). However, if $k_2 \to 0$, the cut degenerates into a Γ shaped curve containing the real axis segment $\zeta = x$, $0 \leq x \leq k_1$ and the entire imaginary axis $\zeta = iy$, $-\infty < y \leq 0$.

The parameterization in (9) however only picks up the imaginary axis when $k_2 = 0$. Consequently, an integral around the portion of the cut on $(0, k_1)$ must be added for correct results,

$$\frac{1}{2}\left[\int_0^{k_1} e^{-ixd} J_1(\beta) H_1^{(2)}(\beta)\,dx + \int_{k_1}^{0} e^{-ixd} J_1(\alpha) H_1^{(2)}(\alpha)\,dx\right]$$

$$\beta = a\sqrt{k_1^2 - x^2} \quad , \quad \alpha = e^{-i\pi}\beta \quad .$$

Again, we use the analytic continuation formulae (6) to get

$$\int_0^{k_1} e^{-ixd} J_1^2(\beta)\,dx \quad , \quad \begin{matrix} \beta = a\sqrt{k_1^2 - x^2} \\ k_2 = 0 \end{matrix} \quad . \tag{11}$$

Notice that this integral is not singular at $x = k_1$ and requires no special treatment for polynomial type integrators. Numerical checks on I_1 and I_2 for $k_2 = 0$ were used to verify the correctness of (11).

References

1. M. Abramowitz and I. A. Stegun, "Handbook of Mathematical Functions," NBS Applied Math Series, 55, U. S. Department of Commerce.
2. D. E. Amos and R. E. Huddleston, CDC 6600 Codes for the Bessel Functions $J_0(z)$ and $J_1(z)$ for Arbitrary Values of Complex z, SLL-73-0262, Sandia Laboratories, July, 1973.
3. J. A. Fuller and J. R. Wait, Mutual Electromagnetic Coupling of Coaxial Loops in a Borehole, Radio Science, Vol. 8, pp 453-457, May, 1973.
4. N. W. McLachlan, "Bessel Functions for Engineers," Oxford University Press, London, 1941.
5. J. S. Yu, Self-Consistent Evaluation of Complex Constitutive Parameters, Accepted for publication IEEE Trans. Antennas and Propagation, 1981.

Distribution:

2355 H. M. Bivens
2646 M. R. Scott
2552 R. D. Moyer
4733 J. S. Yu (5)
4733 C. L. Schuster
4733 P. C. Lysne
5600 D. B. Shuster
Attn: 5610 A. A. Lieber
5620 M. M. Newsom
5630 R. C. Maydew
5640 G. J. Simmons
5641 R. J. Thompson
5641 P. B. Bailey
5642 L. F. Shampine
5642 D. E. Amos (30)
8266 E. A. Aas
8332 T. H. Jefferson
8332 R. E. Huddleston
3141 T. L. Werner (5)
3151 W. L. Garner (3)
For DOE/TIC (Unlim. Release)
3145-3 R. Campbell (25)
For DOE/TIC

Org.	Bldg.	Name	Rec'd by *	Org.	Bldg.	Name	Rec'd by *

* Recipient must initial on classified documents.